FILTER RESPONSE OF RESONANT WAVEGUIDE DIELECTRIC GRATINGS AT PLANE-WAVE CONICAL INCIDENCE

Á. Coves and P. P. Garrido

Departamento de Física Aplicada y de Computadores
Universidad Miguel Hernández
Elche, Alicante 03202, Spain

B. Gimeno and M. V. Andrés

Departamento de Física Aplicada y Electromagnetismo — ICMUV
Universidad De Valencia
C/Dr. Moliner, 50, Burjasot, Valencia 46100, Spain

Abstract—An accurate and efficient formulation is presented for the electromagnetic analysis of dielectric waveguide gratings under plane-wave conical incidence. An arbitrary number of dielectric bars can be placed inside each one-dimension periodic cell, including the effect of dielectric losses. The reflectance of a dielectric waveguide grating under conical incidence is compared with theoretical results presented by other authors, finding a very good agreement. A single-layer reflection filter has been designed centered at $\lambda_0 = 1.5\,\mu$m whose spectral and angular responses are shown. For this structure, the effect of the asymmetry of the distribution of the refraction index in the reflectance has been analyzed, observing a splitting of the reflection peak around the design wavelength. Finally it is discussed the equivalence between a volume grating and a shallow surface-relief grating, providing two examples of designing prescriptions.

1. INTRODUCTION

The scattering of electromagnetic waves in periodic media plays a central role in areas of physics and engineering as antennas technology [1] or the development of artificial magnetic conductors [2].

Corresponding author: B. Gimeno (benito.gimeno@uv.es).

Both cases of one-dimensional [3] and two-dimensional [4–6] periodic structures have been extensively treated in the technical literature.

Multilayered dielectric structures composed by homogeneous layers [7] or containing a periodic variation along any of the dielectric layers [8–12], have been subject of great interest for many years. In such structures, leaky modes can be excited in suitable geometries, producing total reflection at the resonance wavelengths. These guided-mode resonance structures have recently been of considerable interest for optics and microwave applications as passive signal processing devices. Research in this field has the potential of producing a new class of passive elements called resonant waveguide gratings with a large number of applications. A few of these possible uses include static and tunable spectral filters with arbitrarily narrow, controlable linewidths, optical switches and modulators, polarizers, couplers, and many other applications [13–17].

This paper describes the guidance and scattering characteristics of dielectric waveguide gratings at conical incidence (also called three-dimensional incidence), for the general case when the grating wave vector is not contained in the plane of incidence. The analysis extends a previous one [18] by considering an arbitrary number of dielectrics inside the periodic cell in the dielectric grating under plane-wave conical incidence. This formulation is applied to the accurate electromagnetic analysis of the modal spectrum (propagation constant and field distribution) of the modes in lossy dielectric periodic media under three-dimensional plane wave excitation. It must be emphasized that the complexity of the new method proposed in this paper does not increase with the number of dielectric slabs present in the unit cells, such as it usually happens with other classical analysis techniques which are limited however to gratings with special simple groove shapes [19–21]. Furthermore, the presence of losses in the dielectric slabs can be easily considered by simply introducing a complex permittivity in the formulation derived. In addition, it is demonstrated the orthogonality relationship satisfied by such modes in the case of lossless periodic dielectric media.

In order to analyze the reflectance response of a dielectric waveguide grating when a linearly polarized plane-wave is incident on the structure with arbitrary polarization, the linearly polarized plane-wave has been decomposed into the E-Type and H-Type zero order Floquet modes [22]. This decomposition has been particularized for the most usual cases of incidence with TE or TM polarization, i.e., the incident electric field being perpendicular or parallel to the plane of incidence. The spectral response of a waveguide grating under three-dimensional TE incidence is obtained and compared with theoretical

results presented by other authors, finding a very good agreement. Next, making use of the developed analysis method it has been designed a single-layer reflection filter at normal TE incidence centered at $\lambda_0 = 1.5\,\mu$m with symmetrical line shape and low reflectivity out of the resonance. The filter's spectral and angular responses are also shown. For this structure, the effect of the asymmetry of the distribution of the refraction index in the reflection characteristics of the waveguide grating filter has been analyzed. To this end, additional dielectric slabs with different refraction index have been introduced in the unit cell of a symmetric waveguide grating, thus conforming an asymmetric structure, again without increasing the complexity of the formulation developed. The spectral response of this asymmetric configuration shows a splitting of the reflection peak into two new resonances around the original resonant wavelength.

Finally, it is discussed if a given volume grating for optical applications can be replaced by an equivalent surface-relief grating. In particular, the case of volume gratings with small refractive index difference has been considered (this could be accomplished by doping the material), and an equivalent shallow surface-relief grating has been found, which could be prepared by ion or chemical etching of the material. Thus, in the last section two examples of designing prescriptions to find the right equivalent grating are given, and the limitation of this equivalence is discussed.

2. ANALYSIS METHOD

Figure 1 shows the geometry of a dielectric waveguide grating formed by two homogeneous dielectric layers characterized by their refraction index n_h and thicknesses h_h, and a periodic dielectric layer with thickness h_p and period D in the Y direction, formed by several alternating dielectric bars homogeneous in the X axis with refraction index n_{pi} and widths l_i, being $i = 1, 2, 3$ for the case of Fig. 1. An arbitrary number of dielectric bars can be included in the elemental cell. The waveguide grating is illuminated from the air region $z < 0$ by an arbitrary linearly polarized plane-wave with a wave vector given by

$$\mathbf{k} = k_0 \sin\theta \cos\phi\,\widehat{\mathbf{x}} + k_0 \sin\theta \sin\phi\,\widehat{\mathbf{y}} + k_0 \cos\theta\,\widehat{\mathbf{z}} \qquad (1)$$

where $k_0 = \omega\sqrt{\mu_0 \varepsilon_0}$ is the wavenumber in free space, and θ and ϕ are the elevation and azimuthal angles of the three-dimensional incident plane-wave, respectively.

The fields are assumed to have a harmonic time dependence, $\exp(j\omega t)$. Since the material in each dielectric layer is homogeneous along the Z direction, the propagating modes in this direction have
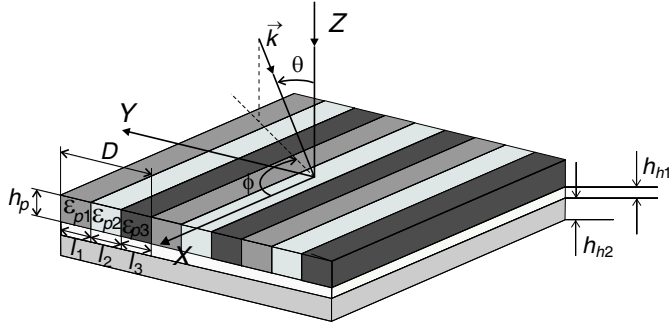
Figure 1. Scheme of a volume grating composed of two homogeneous dielectric layers and one periodic dielectric layer with periodicity D in the Y direction, formed by three alternating dielectric bars homogeneous in the X axis.

an exponential dependence $\exp(-j\beta z)$, where β is the propagation constant. Following the procedure described in a previous work [18], the modes in the homogeneous regions employed in this work are the well known Floquet harmonics with E-Type or TM^y polarization (denoted as $'$), and H-Type or TE^y polarization (denoted as $''$), which are described as follows

$$\tilde{\mathbf{e}}_p^{'h} = \frac{1}{\sqrt{D}\beta_{h_p}\omega\varepsilon_h} e^{-j(k_x x + k_{y_p} y)} \left[-k_x k_{y_p}\widehat{\mathbf{x}} + \left(k_h^2 - k_{y_p}^2 \right)\widehat{\mathbf{y}} \right] \quad (2)$$

$$\tilde{\mathbf{h}}_p^{'h} = \frac{-1}{\sqrt{D}} e^{-j(k_x x + k_{y_p} y)}\widehat{\mathbf{x}} \quad (3)$$

$$\tilde{\mathbf{e}}_p^{''h} = \frac{\omega\mu\beta_{h_p}}{\sqrt{D}\left(k_h^2 - k_{y_p}^2 \right)} e^{-j(k_x x + k_{y_p} y)}\widehat{\mathbf{x}} \quad (4)$$

$$\tilde{\mathbf{h}}_p^{''h} = \frac{1}{\sqrt{D}} e^{-j(k_x x + k_{y_p} y)} \left[\frac{-k_x k_{y_p}}{\left(k_h^2 - k_{y_p}^2 \right)}\widehat{\mathbf{x}} + \widehat{\mathbf{y}} \right] \quad (5)$$

where $\varepsilon_h = \varepsilon_{rh}\varepsilon_0 = n_h^2\varepsilon_0$, $k_h = k_0\sqrt{\varepsilon_{rh}}$, $k_x = k_0\sin\theta\cos\phi$, $\beta_{h_p} = \sqrt{k_h^2 - k_x^2 - k_{y_p}^2}$ and k_{y_p} is the Floquet wavenumber, given by

$$k_{y_p} = k_0\sin\theta\sin\phi + \frac{2\pi}{D}p \ ; \ \ p = 0, \pm 1, \pm 2, \ldots \quad (6)$$

The modes in the periodic regions are obtained using a vectorial modal method previously developed in [23–25] for one-dimensional

gratings, and in [4, 6] for the two-dimensional case. The mentioned technique has been extended in this contribution for considering an arbitrary number of dielectrics inside the periodic cell under conical incidence excitation. In this method, the vector wave equation satisfied by the transverse components of the magnetic field in the periodic medium is expressed as an eigenvalue problem shown next

$$\left[\nabla_t^2 + k_0^2 \varepsilon_r + \left(\frac{\nabla_t \varepsilon_r}{\varepsilon_r}\right) \times (\nabla_t \times \circ)\right] \mathbf{h}_n = \beta_n^2 \mathbf{h}_n \;\; \Rightarrow \;\; L\mathbf{h}_n = \beta_n^2 \mathbf{h}_n \quad (7)$$

where L represents the differential operator governing the evolution of the transverse magnetic field of the n-th mode along the Z axis, β_n is the propagation constant of such mode, and ε_r is the complex relative permittivity of the medium (note that $\varepsilon_r = \varepsilon_r(y)$). It should be emphasized that the use of a complex dielectric permittivity allows to account in a rigorous manner (non-perturbative) the presence of ohmic losses in the dielectric media. Following the well-known Method of Moments [26], this eigenvalue equation can be expressed in a matrix form if the modes in the periodic medium are expanded in terms of an auxiliary basis whose modes satisfy an orthogonality relationship of the form

$$\left\langle \tilde{\mathbf{e}}_p | \tilde{\mathbf{h}}_q \right\rangle = \delta_{pq} \quad (8)$$

where δ_{pq} is the Kronecker delta function. In the present formulation, the modes corresponding to a homogeneous medium (Eqs. (2)–(5)) of relative dielectric permittivity $\tilde{\varepsilon}_{rb}$ have been used as auxiliary basis functions. Such modes have been adequately normalized according to

$$\left\langle \tilde{\mathbf{e}}_p | \tilde{\mathbf{h}}_q \right\rangle = \int_{CS} \left(\tilde{\mathbf{e}}_p^* \times \tilde{\mathbf{h}}_q \right) \times \hat{\mathbf{z}} \, dS = \delta_{pq} \quad (9)$$

where CS represents in this case the cross section of the periodic cell (* represents the complex conjugate operation). The next step in the application of the Method of Moments is the expansion of the fields in terms of the auxiliary basis modes,

$$\mathbf{h}_n = \sum_q c_{qn} \tilde{\mathbf{h}}_q \quad (10)$$

where c_{qn} are the complex coefficients of the modal expansion for the transverse magnetic field of the n-th mode. Finally, the last step in the application of the Method of Moments yields to the following linear matrix eigenvalue problem:

$$\sum_q L_{pq} c_{qn} = \beta_n^2 c_{pn} \quad (11)$$

where L_{pq} are the matrix elements of the L operator, which are obtained as follows:

$$L_{pq} = \langle \tilde{\mathbf{e}}_p | L \tilde{\mathbf{h}}_q \rangle = \int_{CS} \left(\tilde{\mathbf{e}}_p^* \times L \, \tilde{\mathbf{h}}_q \right) \times \hat{\mathbf{z}} \, dS \; . \qquad (12)$$

The $[L]$ matrix is infinitely-dimensional in the theory described above when all the modes are included. In order to develop a realistic method, it is necessary to work with a finite set of well-known auxiliary fields to expand the modes in each periodic dielectric layer in terms of the auxiliary basis modes. Therefore, numerical convergence tests must be done by considering the number of auxiliary modes over meaningful ranges, thus studying the stability of the solutions.

For the particular case of a one-dimensional periodic dielectric medium with an arbitrary number of dielectrics inside the periodic cell, the matrix elements of the L operator have been analytically calculated [18]. From them, it can be easily noticed that the coupling terms between E-Type and H-Type modes disappear for non-conical incidence ($\phi = 90°$ or $k_x = 0$), as it should be expected from previous reported analysis [25, 27]. The numerical diagonalization of (11) yields the propagation constants as well as the magnetic fields of the modes in the periodic medium at each frequency point. Finally, the transverse electric fields of the modes are related to the magnetic ones through constraints directly derived from Maxwell's equations [28].

In general, the modes in a periodic medium are not a conventional orthogonal basis. But in the particular case of a lossless periodic dielectric medium it has been found that the modes in such a medium also satisfy an orthogonality relation of the form given in (9),

$$\int_{CS} \left(\mathbf{e}_p^* \times \mathbf{h}_q \right) \times \hat{\mathbf{z}} \, dS = \delta_{pq} \qquad (13)$$

which can be easily derived from Maxwell's equations and the Floquet's theorem, as it is demonstrated in the Appendix A.

After specifying the fields in all homogeneous and periodic regions of the structure, the scattering parameters are obtained by imposing the boundary conditions between adjacent layers, obtaining the Generalized Scattering Matrix (GSM) at each interface between adjacent layers of the structure, i.e., the amplitudes of the reflected and the transmitted modes. Then, the GSM of the global structure is constructed by means of the cascaded connection of the individual GSMs of the interfaces, and the scattering matrices corresponding to the propagation through the layers, following the technique described by T. S. Chu [29]. The global GSM technique yields the amplitudes of the scattered modes reflected and transmitted by the structure,

considering an incident plane wave with a unit amplitude and with either E-Type or H-Type polarization.

In order to analyze the 3D scattering of a linearly polarized plane-wave incident on a dielectric waveguide grating, the linearly polarized plane-wave is decomposed into a linear combination of E-Type ($'$) and H-Type ($''$) zero order modes. This decomposition has been particularized to the most usual cases of incidence with TE or TM polarization, i.e., the incident electric field being perpendicular or parallel to the plane of incidence, respectively.

In the described method for obtaining the scattering parameters of the problem, the multimode scattering matrix of the structure is infinitely-dimensional. In order to reduce the scattering problem to a computationally suitable form, the individual layer multimode scattering matrices were truncated at a finite size. Such a size must be large enough to allow for an accurate calculation of the scattered (reflected and transmitted) modes which are significant in the overall solution, but small enough for computational efficiency issues. As a consequence, both propagating and non-propagating (or evanescent) modes are included in the GSM formulation. For each particular case, a study of convergence must be also performed in order to reach an accurate solution for the scattering parameters of the overall structure.

3. NUMERICAL RESULTS

In order to test the developed algorithm, the modal spectrum of an infinite periodic dielectric medium under three-dimensional plane-wave excitation is first examined, with two dielectric slabs within the unit cell with the following parameters: $D = 0.6\,\lambda_0$, $n_{p1} = 1.0$, $n_{p2} = 1.6$, $l_1/D = 0.5676$, $l_2/D = 0.4324$, $\lambda_0 = 1.55\,\mu\text{m}$. In the calculations the auxiliary system used was an infinite homogeneous dielectric medium with $\tilde{\varepsilon}_{rb} = 1.0$. For this example the convergence (in this case a 0.5% of relative error) is reached with only 30 modes of the auxiliary basis, taking 0.01 seconds per frequency point (in a PentiumIV@2.4 GHz processor). Fig. 2 shows the normalized electric field distribution of the first (a) and second (b) modes along the characteristic cell of this medium under three-dimensional plane wave excitation with $\theta = 45°$, $\phi = 60°$. It can be observed that the first mode has an H-Type structure, because the e_y component is nearly zero for this mode. For the second mode, it can also be appreciated that the tangential component to the dielectric discontinuity (e_x component) in continuous in the plane of the discontinuity, while the normal component to the dielectric discontinuity, which corresponds to e_y, is discontinuous in this plane.
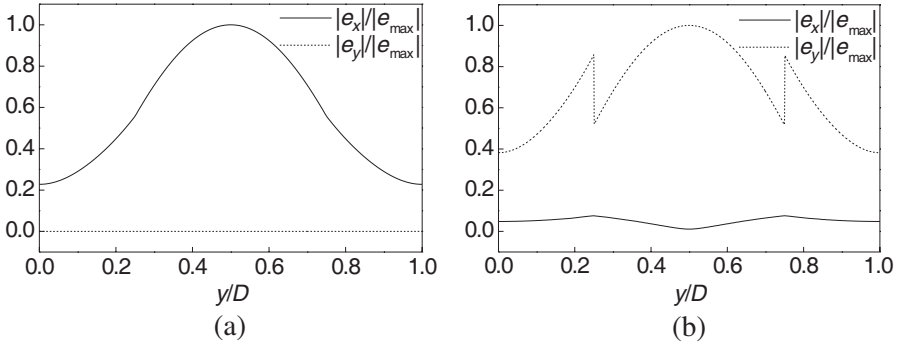
Figure 2. Distribution of the normalized transverse electric field for the first (a) and second (b) modes along the characteristic cell of an infinite periodic dielectric medium under three-dimensional plane wave excitation at $\theta = 45°$, $\phi = 60°$, with two dielectric slabs within the unit cell with the following parameters: $D = 0.6\lambda_0$, $n_{p1} = 1.0$, $n_{p2} = 1.6$, $l_1/D = 0.5676$, $l_2/D = 0.4324$, $\lambda_0 = 1.55\,\mu m$.

In the next example numerical studies of the spectral response of a dielectric waveguide grating at conical incidence have been carried out and compared to theoretical results obtained by other authors. The problem under analysis is a periodic dielectric grating placed between air ($n_a = 1.0$) and a dielectric substrate with refraction index $n_s = 3.5$ (see Fig. 3). This structure was designed in [19] to be antirreflecting for use at $\lambda_0 = 1.55\,\mu m$ when it is illuminated by a plane wave with TE polarization at normal incidence ($\phi = 90°$, which means in this case that the electric field is parallel to the X axis). The periodic layer of thickness $h = 0.401\lambda_0$ is formed by two dielectric slabs within the unit cell, with $n_{p1} = 3.5$, $n_{p2} = 1.0$ and $l_1/D = 0.222$, $l_2/D = 0.778$. In Fig. 3 it is shown the reflection power coefficient of the structure (or reflectance, which is denoted as R), under TE illumination at $\theta = \phi = 45°$ as a function of the wavelength-to-period ratio; our results are compared to those calculated by other authors [19], showing an excellent agreement.

Next, making use of the developed method and applying the guided-mode resonance properties of planar dielectric waveguide gratings [10, 30], a single-layer reflection filter has been designed centered at $\lambda_0 = 1.5\,\mu m$, with symmetrical line shape and near-zero reflectivity over appreciable wavelength bands adjacent to the resonance wavelength. The filter is based on a single-layer waveguide grating surrounded by air which is illuminated by a plane-wave under normal TE incidence ($\phi = 90°$), with the following parameters (which
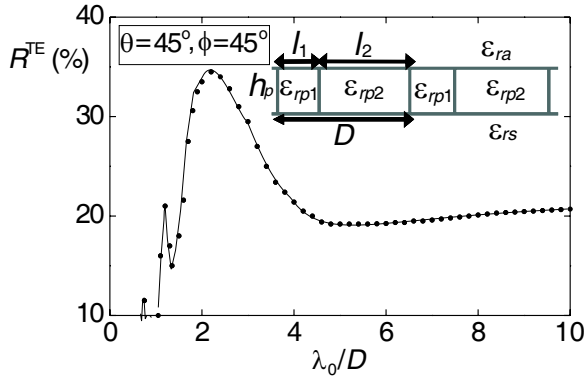
Figure 3. Reflectance (R) of a dielectric grating under TE plane-wave excitation at $\theta = \phi = 45°$ and $\lambda_0 = 1.55\,\mu\text{m}$ as a function of the wavelength-to-period ratio. Parameters of the problem: $h_p = 0.401\lambda_0$, $n_{p1} = 3.5$, $n_{p2} = 1.0$, $l_1/D = 0.222$, $l_2/D = 0.778$, $n_a = 1.0$, $n_s = 3.5$. Results obtained with the presented technique are represented with solid line, in comparison with those presented in [19] showed with dots.
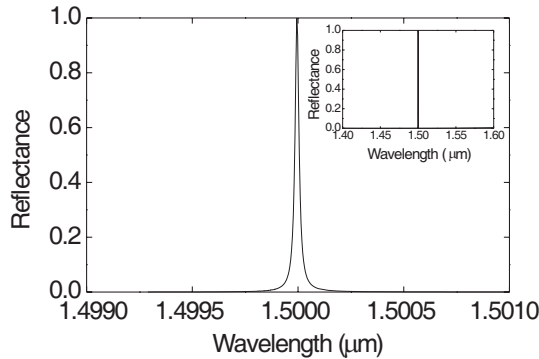

Figure 4. TE spectral response of a waveguide-grating filter centered at $\lambda_0 = 1.5\,\mu\text{m}$. The filter is based on a single-layer waveguide grating surrounded by air which is illuminated by a plane-wave under normal TE incidence, with the following parameters: $D = 1.17\,\mu\text{m}$, $h_p = 0.5\,\mu\text{m}$, $n_{p1} = 1.49$, $n_{p2} = 1.5$, $l_1/D = l_2/D = 0.5$.

satisfy the phase-match condition described in [18, 25] in the grating at the resonance wavelength): $D = 1.17\,\mu\text{m}$, $n_{p1} = 1.49$, $n_{p2} = 1.5$, $l_1/D = l_2/D = 0.5$, $h = 0.5\,\mu\text{m}$. Fig. 4 shows the spectral behavior of the waveguide grating around the resonance. Only the zero

order Floquet mode propagates in air regions (all higher-order modes are evanescent). Note that the waveguide grating filter produces a symmetric spectral response in reflection with almost zero reflectance over appreciable wavelength bands adjacent to the resonance peak (as it can be also observed in the inset of Fig. 4). In Fig. 5 it is shown the reflectance of this layer under conical plane-wave incidence at two different wavelengths of (a) $1.5\,\mu m$ (resonance wavelength), and (b) $1.505\,\mu m$ (out of resonance). In Fig. 5(a) it can be observed the rapid decrease of the reflection filter reflectance when the direction of incidence is shifted from the design value $\theta = 0°$ (the reflectance rapidly changes from 1 to 0), while the dependence with ϕ is smooth. Moreover, in Fig. 5(b) it can be appreciated that out of the design wavelength, when $\lambda_0 = 1.505\,\mu m$, the directions of incidence that excite a resonance move apart from the normal incidence. In this case, we can observe that the resonance has moved from $\theta = 0°$, $\phi = 90°$ to $\theta \sim 0.29°$ when $\phi \in [70°–90°]$.

For the filter designed in Fig. 4, it has been analyzed the effect of the asymmetry of the distribution of the refraction index with respect to the center of the periodic cell in the reflectance of the structure. To this end, it has been studied the spectral response of a dielectric waveguide grating with the same thickness, periodicity and average refraction index of the previous filter (see Fig. 4), but with three dielectric materials in the periodic cell, being $n_{p1} = 1.49$, $n_{p2} = 1.495$, $n_{p3} = 1.5$, $l_1 = l_2 = l_3 = D/3$. Thus, an additional
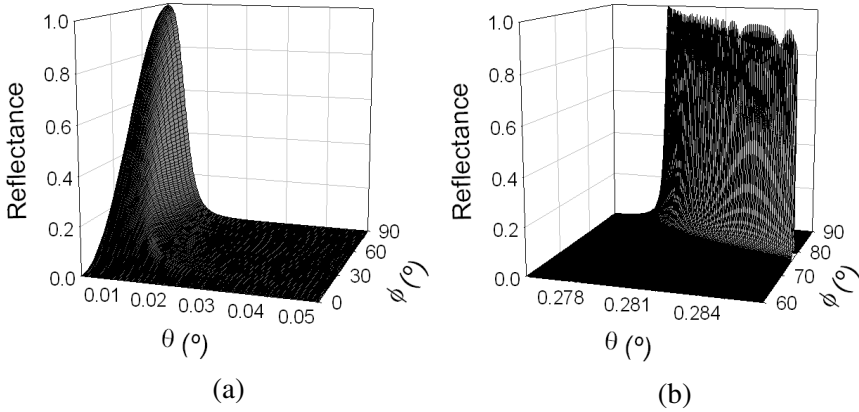

(a)

(b)
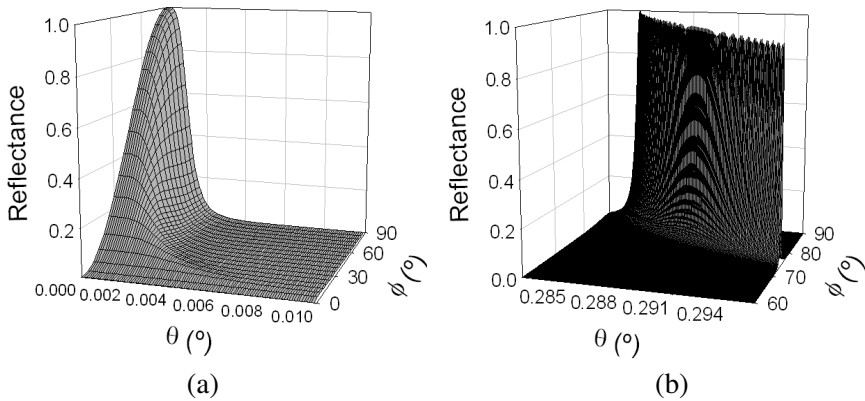
Figure 5. Reflection coefficient $R(\theta, \phi)$ of the grating of Fig. 4 for TE conical plane-wave incidence, at two different wavelengths of (a) $1.5\,\mu m$ (resonance wavelength) and (b) $1.505\,\mu m$ (out of resonance).

dielectric slab in the unit cell of the symmetric waveguide grating of Fig. 4 has been introduced conforming an asymmetric structure. The reflectivity of this new filter under normal TE incidence is represented in Fig. 6, where it is observed a splitting of the reflection peak into two new resonance peaks at $1.499\,\mu$m and $1.501\,\mu$m respectively. The splitting of the reflection peak is associated with the rupture of degeneracy of the $+1$ and -1 leaky-wave modes excited in the waveguide grating due to the asymmetry of the relative permittivity distribution with respect to the center of the periodic cell, which was already observed in previous works [31–33]. In order to study this phenomenon, the effect of introducing an additional dielectric in a symmetric configuration in the unit cell of the waveguide grating of Fig. 4 has been analyzed, obtaining a new symmetric reflection filter with the same period, thickness and average refraction index than the one described above, but with the following distribution of refraction index along the periodic cell: $n_{p1} = n_{p5} = 1.49$, $n_{p2} = n_{p4} = 1.4975$, $n_{p3} = 1.5$, and $l_1 = l_2 = l_3 = l_4 = l_5 = D/5$. The spectral response obtained in this case is identical to that shown in Fig. 4 and has been omitted because of brevity (the waveguide grating also presents a unique resonance peak at $\lambda_0 = 1.5\,\mu$m). For the three bar asymmetric case a 3D plot representing the reflectance of the grating for TE conical incidence is included in Fig. 7, at two different wavelengths of (a) $1.501\,\mu$m (second resonance wavelength) and (b) $1.505\,\mu$m. In Fig. 7(a) the selectivity of the reflection filter is shown when the direction of incidence is shifted from the design value at normal incidence ($\theta = 0°$,
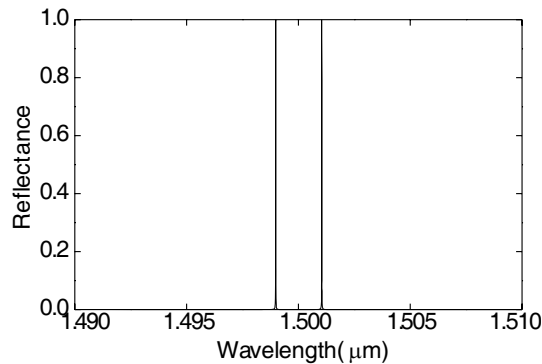
Figure 6. TE spectral response of a single-layer waveguide grating with three dielectrics in the periodic cell surrounded by air with the following parameters: $D = 1.17\,\mu$m, $h_p = 0.5\,\mu$m, $n_{p1} = 1.49$, $n_{p2} = 1.495$, $n_{p3} = 1.5$, $l_1 = l_2 = l_3 = D/3$, $\theta = 0°$.

Figure 7. Reflection coefficient $R(\theta, \phi)$ of the grating of Fig. 6 for TE conical plane-wave incidence, at two different wavelengths of (a) 1.501 μm (second resonance wavelength) and (b) 1.505 μm.

$\phi = 90°$). It can be observed that the reflectance changes rapidly from 1 to 0 as a function of θ, while the response is smooth as a function of ϕ. Furthermore, it can be appreciated in Fig. 7(b) that out of the resonance wavelength, the resonance moves to $\theta \sim 0.28°$ when $\phi \in [70°$–$90°]$.

## 4. ANALYSIS OF SHALLOW SURFACE-RELIEF DIELECTRIC GRATINGS

Dielectric waveguide gratings may present difficulties in their manufacturing technological process when applied in the optical frequency range. From a practical point of view, the physical implementation of the described reflection filter, centered around 1.5 μm, could be performed by using silica as the high refraction index material ($n_{p1}(\text{SiO}_2) = 1.5$), and doped silica as the low refraction index one (with $n_{p2} = n_{p1} - \delta$, being $\delta = 0.01$). In this section, it is analyzed the use of an equivalent reflection filter manufactured engraving periodic shallow grooves over the surface of an homogeneous dielectric layer of refraction index $n = 1.5$ (see the inset in Fig. 8), which could be manufactured using a combination of photolithographic and, etching techniques and conformal coatings. The depth of the groove t necessary for obtaining the same resonance wavelength in a given modulated periodic structure depends on the modulation of the refraction index of the waveguide grating filter.

The analysis of the surface-relief grating has been carried out considering that the structure is the combination of a homogeneous layer with a thickness h-t and refractive index n_{p1}, and that on top of it, a periodic layer of thickness t and refraction index values of 1 and n_{p1} is placed. For the symmetrical reflection filter at normal incidence considered above in Fig. 4 (whose thickness is $h = 0.5\,\mu$m), Fig. 8 shows the variation of the relative groove depth t/h of an equivalent surface-relief grating which provides the same resonance wavelength than the modulated periodic layer ($\lambda_0 = 1.5\,\mu$m), as a function of the modulation of the refraction index in the periodic cell ($(n_{p1}-n_{p2})/n_{p1}$). Thus, a surface-relief grating with an adequate depth can give the same spectral response as the waveguide grating filter for normal incidence.

We are interested in predicting the groove depth which provides the same spectral response than an equivalent periodic grating. For the case analyzed in Fig. 8, a quasi-linear dependence of the relative groove depth t/h has been observed with respect to the modulation of the refraction index over the range of modulation analyzed, whose linear fit is shown in this figure. Nevertheless, the results of a similar study are shown in Fig. 9 for another dielectric material of higher refraction index $n_{p1} = 1.92$. Again, it can be observed a linear dependence of the relative groove depth with respect to the modulation of the refraction index, showing the linear fit a lower slope in this case. In fact, the higher the refraction index of the surface-relief grating, the lower the slope in the linear fit observed. This tendency can be explained using a variational theory [34] for the resonance condition detailed in [12]
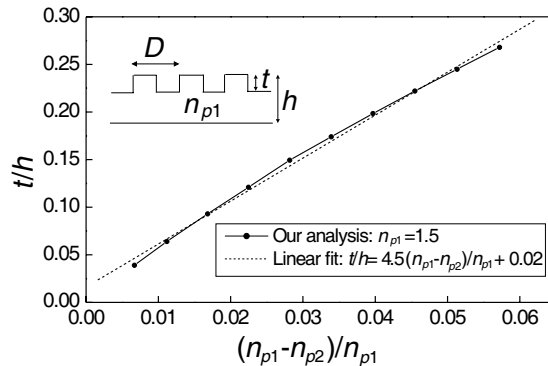
Figure 8. Study of the equivalence between a given modulated periodic structure and an equivalent surface-relief grating providing the same resonance wavelength, corresponding to a dielectric material with $n_{p1} = 1.5$.
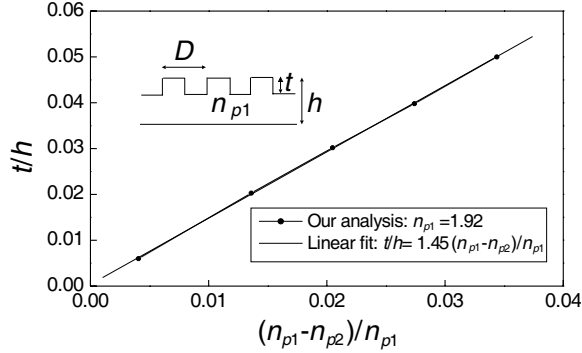
Figure 9. Study of the equivalence between a given modulated periodic structure and an equivalent surface-relief grating providing the same resonance wavelength, corresponding to a dielectric material with $n_{p1} = 1.92$.

for both gratings, and making equal the resonance wavelength in the modulated periodic layer and in the equivalent surface-relief grating. The same resonance condition in both equivalent structures is achieved if the wave vector in the direction of periodicity β_g of the waveguide grating is also the same. Following a scalar approximation for the modes in a periodic grating [34], the wave vector in the perturbed problem (periodic layer with modulation of the refraction index δ or surface-relief grating with relative groove depth t/h) β_g can be approximated as follows

$$\beta_g = \beta_h + k_0 \frac{\int_S (n - n_h)\Psi^2 dS}{\int_S \Psi^2 dS} \tag{14}$$

where S is the waveguide cross section, β_h is the wave vector of an unperturbed problem consisting of an homogeneous dielectric layer of refraction index $n_h = n_{p1}$ and width h, and Ψ is the transverse component of the electric field in the perturbed problem, i.e., in the periodic grating. Then, if the periodic modulated layer and the surface-relief grating must have the same wavevector β_g, it implies that

$$\int_0^h (n_{p2} - n_{p1})\Psi^2 dz = \int_0^t (1 - n_{p1})\Psi^2 dz \;. \tag{15}$$

If we approximate Ψ inside the grating by a uniform field we obtain

$$(n_{p2} - n_{p1})\Psi^2 \int_0^h dz = (1 - n_{p1})\Psi^2 \int_0^t dz \Rightarrow (n_{p2} - n_{p1})h = (1 - n_{p1})t, \tag{16}$$

or

$$t/h = \frac{n_{p1}}{n_{p1} - 1} \frac{(n_{p1} - n_{p2})}{n_{p1}} . \tag{17}$$

This approximation yields a slope of 3.0 for the first material analyzed of $n_{p1} = 1.5$, and a slope of 2.09 for the second material of $n_{p1} = 1.92$. This approximation provides the same tendency for the slope of the linear fit in Fig. 8 and Fig. 9 obtained with a rigorous analysis. However, a rigorous study must be performed at each particular case to obtain the right equivalence.

Finally, it has been studied the reflectance at conical plane-wave incidence of the equivalent surface-relief dielectric grating with a groove depth of $t = 0.02\,\mu$m, which provides the same resonance wavelength of the modulated periodic layer of Fig. 4 at normal TE incidence. The analysis has been carried out at two different wavelengths: (a) $1.5\,\mu$m (resonance wavelength) and (b) $1.505\,\mu$m (out of resonance). In Fig. 10(a) it can be checked that this equivalent surface-relief grating shows total reflection at normal incidence, as it was also observed for
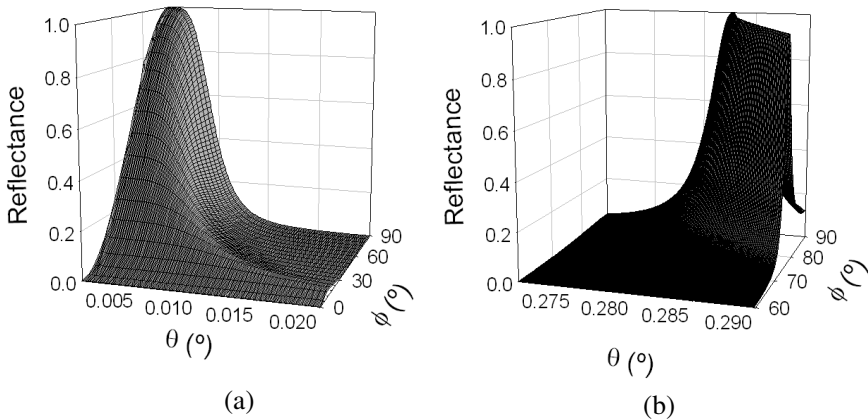
Figure 10. Reflection coefficient $R(\theta, \phi)$ of a surface-relief grating with a groove depth of $t = 0.02\,\mu$m, equivalent to the modulated periodic layer of Fig. 4, for TE conical incidence, at two different wavelengths of (a) $1.5\,\mu$m (resonance wavelength) and (b) $1.505\,\mu$m (out of resonance).

the modulated periodic layer in Fig. 5(a), although a slightly less sharp dependence with θ can be observed. In Fig. 10(b) it can be appreciated that out of the design wavelength, the resonance moves to $\theta \sim 0.29°$ when $\phi \in [70°\text{–}90°]$, as it happens in Fig. 5(b), but with a smoother angular dependence on both θ and ϕ.

5. CONCLUSION

In this work it is presented a formulation for the rigorous electromagnetic analysis of plane-wave diffraction by one-dimensional periodic dielectric gratings under the most general condition of conical incidence (three-dimensional incidence). In each elemental periodic cell an arbitrary number of losses dielectric slabs can be inserted. The propagation constant and the fields in a one-dimensional periodic dielectric medium are determined as the numerical solution of a linear eigenvalue problem. The scattering parameters of the dielectric grating are then obtained by imposing the boundary conditions in terms of the GSM formulation. The developed theory has been tested for conical incidence by comparison to numerical results previously obtained by other authors, showing an excellent agreement. As an example, making use of the guided-mode resonance properties of planar dielectric waveguide gratings, a symmetrical reflection filter at normal TE incidence has been designed using two dielectric materials in the periodic cell for a central wavelength of $\lambda_0 = 1.5\,\mu\text{m}$, showing near-zero reflectivity over appreciable wavelength bands adjacent to the resonance wavelength. For this filter, it is shown the effect of varying both angles θ and ϕ in the reflectance response of the structure at two different wavelengths. It has been analyzed the effect of the asymmetry of the relative permittivity distribution with respect to the center of the periodic cell for this filter at normal TE incidence, observing a splitting of the reflection peak into two resonance peaks around the resonance wavelength predicted by the classical phase-match condition. Finally, a study of the equivalence between a given modulated periodic structure and an equivalent shallow surface-relief grating providing the same resonance wavelength has been performed, showing a linear dependence of the relative groove depth t/h with respect to the modulation of the refraction index in the equivalent modulated grating. Our conclusion is that the slope of the linear fit depends on the refraction index of the surface-relief grating, which implies that a study of this dependence must be performed at each particular case.

APPENDIX A. ORTHOGONALITY RELATIONSHIP IN A LOSSLESS PERIODIC DIELECTRIC MEDIUM

In this appendix, the orthogonality relationship satisfied by the modes in a lossless periodic dielectric medium is demonstrated. Following the same procedure described by Collin [28] for a shielded guide, let $\mathbf{H}_{tn}$, $\mathbf{E}_{tn}$ and $\mathbf{H}_{tm}$, $\mathbf{E}_{tm}$ be the transverse fields for two linearly independent solutions of Maxwell's equations in a lossless periodic dielectric medium. The curl equations for the electric field of the n-th mode and its conjugate for the m-th mode are given by

$$\nabla \times \mathbf{E}_n = -j\omega\mu\mathbf{H}_n \tag{A1}$$
$$\nabla \times \mathbf{E}_m^* = j\omega\mu\mathbf{H}_m^* \tag{A2}$$

where $\mathbf{H}_n$, $\mathbf{E}_n$ and $\mathbf{H}_m$, $\mathbf{E}_m$ are the total fields, i.e., both the transverse and axial components. Scalar multiplying the above equations by $\mathbf{H}_m^*$ and $\mathbf{H}_n$, respectively, and adding gives

$$\mathbf{H}_m^* \times \nabla \times \mathbf{E}_n + \mathbf{H}_n \times \nabla \times \mathbf{E}_m^* = 0 \,. \tag{A3}$$

Scalar multiplying the curl equations for $\mathbf{H}_n$, $\mathbf{H}_m^*$ by $\mathbf{E}_m^*$, $\mathbf{E}_n$ and adding gives a similar result in a lossless dielectric media ($\varepsilon_r = \varepsilon_r^*$), but with the roles of $\mathbf{E}$ and $\mathbf{H}$ interchanged,

$$\mathbf{E}_m^* \times \nabla \times \mathbf{H}_n + \mathbf{E}_n \times \nabla \times \mathbf{H}_m^* = 0 \,. \tag{A4}$$

Subtracting these equations we obtain the following relationship: $\nabla \times (\mathbf{E}_n \times \mathbf{H}_m^* + \mathbf{E}_m^* \times \mathbf{H}_n) = 0$. Now, making use of the relation $\nabla = \nabla_t + \widehat{\mathbf{z}}\, \partial/\partial z$, and using the two-dimensional form of the divergence theorem, we obtain

$$\oint_C \mathbf{n} \times (\mathbf{E}_n \times \mathbf{H}_m^* + \mathbf{E}_m^* \times \mathbf{H}_n)\, dl$$
$$= j(\beta_n - \beta_m) \int_{CS} \widehat{\mathbf{z}} \times (\mathbf{E}_{tn} \times \mathbf{H}_{tm}^* + \mathbf{E}_{tm}^* \times \mathbf{H}_{tn})\, dS \tag{A5}$$

where CS represents the cross section of the periodic cell and C represents the contour of the cell. It can be easily proven that the contour integral vanishes since it can be decomposed into four line integrals: on one hand, the two line integrals for constant x coordinate are identical in a medium not dependent on x, but with a sign reversal due to the inversion in the direction of integration, so both terms cancel each other; on the other hand, the line integrals along the lines $y = y_0$ and $y = y_0 + D$ also cancel each other, because the fields only differ in

a phase term, given by the Floquet's theorem:

$$\mathbf{E}_{tn}(y_0 + D) = \mathbf{E}_{tn}(y_0)e^{-jk_{yn}D} \tag{A6}$$

$$\mathbf{H}_{tn}(y_0 + D) = \mathbf{H}_{tn}(y_0)e^{-jk_{yn}D} \tag{A7}$$

Nevertheless, the above mentioned phase terms cancel when substituting the fields in the line integrals, so finally these line integrals also cancel each other. Thus, we obtain

$$j(\beta_n - \beta_m) \int_{CS} \widehat{\mathbf{z}} \times (\mathbf{E}_{tn} \times \mathbf{H}_{tm}^* + \mathbf{E}_{tm}^* \times \mathbf{H}_{tn})\, dS = 0 \tag{A8}$$

It is convenient to write the expression for the transverse fields in the following form

$$\mathbf{H}_{tn} = \mathbf{h}_n(x,y)e^{-j\beta_n z} \tag{A9}$$

$$\mathbf{E}_{tn} = \mathbf{e}_n(x,y)e^{-j\beta_n z} \tag{A10}$$

where $\mathbf{h}_n$, $\mathbf{e}_n$ are the transverse modal vector functions of the transverse coordinates x, y. Introducing these expressions in (A8) we obtain

$$j(\beta_n - \beta_m) \int_{CS} \widehat{\mathbf{z}} \times (\mathbf{e}_n \times \mathbf{h}_m^* + \mathbf{e}_m^* \times \mathbf{h}_n)dS = 0 \tag{A11}$$

since the common exponential terms can be cancelled. To show that each term is equal to zero separately, we consider two solutions $\mathbf{E}_n, \mathbf{H}_n$ and $\mathbf{E}'_m, \mathbf{H}'_m$, where $\mathbf{E}'_m, \mathbf{H}'_m$ is the same mode considered previously, but depending on z according to $\exp(+j\beta_m z)$ rather than $\exp(-j\beta_m z)$. This corresponds to a reversal in the direction of propagation, and, consequently, the direction of the transverse magnetic field is reversed; that is, $\mathbf{E}'_{tm} = \mathbf{e}_m \exp(+j\beta_m z)$, $\mathbf{H}'_{tm} = -\mathbf{h}_m \exp(+j\beta_m z)$. The equation corresponding to Eq. (A11) is now given by

$$j(\beta_n + \beta_m) \int_{CS} \widehat{\mathbf{z}} \times (\mathbf{e}_n \times (-\mathbf{h}_m^*) + \mathbf{e}_m^* \times \mathbf{h}_n)dS = 0 \tag{A12}$$

Addition of (A11) and (A12) gives

$$\int_{CS} (\mathbf{e}_m^* \times \mathbf{h}_n) \times \widehat{\mathbf{z}}\, dS = 0\,, \qquad m \neq n \tag{A13}$$

which is the desired orthogonality relationship satisfied by the non-degenerate modes in a lossless periodic dielectric medium (see (13)).

REFERENCES

1. Pirhadi, A., F. Keshmiri, M. Hakkak, and M. Tayarani, "Analysis and design of dual band high directivity EBG resonator antenna using square loop FSS as superstrate layer," *Progress In Electromagnetics Research*, PIER 70, 1–20, 2007.

2. Hosseini, M., A. Piradi, and M. Hakkak, "A novel AMC with little sensitivity to the angle of incidence using 2-layer jerusalem cross FSS," *Progress In Electromagnetics Research*, PIER 64, 43–51, 2006.

3. Ohki, M., K. Sato, M. Matsumoto, and S. Kozaki, "T-matrix analysis of electromagnetic wave diffraction from a dielectric coated fourier grating," *Progress In Electromagnetics Research*, PIER 53, 91–108, 2005.

4. Attiya, A. M. and A. A. Kishk, "Modal analysis of a two-dimensional dielectric grating slab excited by an obliquely incident plane wave," *Progress In Electromagnetics Research*, PIER 60, 221–243, 2006.

5. Khalaj-Amirhosseini, M., "Scattering of inhomogeneous two-dimensional periodic dielectric gratings," *Progress In Electromagnetics Research*, PIER 60, 165–177, 2006.

6. Attiya, A. M., A. A. Kishk, and A. W. Glisson, "Analysis of two-dimensional magneto-dielectric grating slab," *Progress In Electromagnetics Research*, PIER 74, 195–216, 2007.

7. Oraizi, H. and M. Afsahi, "Analysis of planar dielectric multilayers as FSS by transmission line transfer matrix method (TLTMM)," *Progress In Electromagnetics Research*, PIER 74, 217–240, 2007.

8. Hessel, A. and A. A. Oliner, "A new theory of Wood's anomalies on optical gratings," *Appl. Opt.*, Vol. 10, 1275–1297, 1965.

9. Moharam, M. G. and T. K. Gaylord, "Rigorous coupled-wave analysis of planar-grating diffraction," *J. Opt. Soc. Am.*, Vol. 71, 811–818, 1981.

10. Wang, S. S., R. Magnusson, J. S. Bagby, and M. G. Moharam, "Guided-mode resonances in planar dielectric-layer diffraction gratings," *J. Opt. Soc. Am. A*, Vol. 8, 1470–1475, 1990.

11. Marcuse, D., *Theory of Dielectric Optical Waveguides*, 2nd edition, Academic, New York, 1991.

12. Bertoni, H. L., L. S. Cheo, and T. Tamir, "Frequency-selective reflection and transmission by a periodic dielectric layer," *IEEE Trans. Antennas Propag.*, Vol. 37, 78–83, 1989.

13. Tibuleac, S., R. Magnusson, T. A. Maldonado, P. P. Young,

and T. R. Holzheimer, "Dielectric frequency-selective structures incorporating waveguide gratings," *IEEE Trans. Microwave Theory Tech.*, Vol. 4, 553–561, 2000.

14. Boye, R. R., R. W. Ziolkowski, and R. K. Kostuk, "Resonant waveguide-grating switching device with nonlinear optical material," *Appl. Opt.*, Vol. 38, 5181–5185, 1999.

15. Sharon, A., D. Rosenblatt, A. A. Friesem, H. G. Weber, H. Engel, and R. Steingrueber, "Light modulation with resonant grating-waveguide structures," *Opt. Lett.*, Vol. 21, 1564–1566, 1996.

16. Neviere, M., P. Vincent, R. Petit, and M. Cadilhac, "Systematic study of resonance of holographic thin film couplers," *Opt. Commun.*, Vol. 9, 48–53, 1973.

17. Li, L., "Analysis of planar waveguide grating coupler with double surface corrugations of ideal period," *Opt. Commun.*, Vol. 114, 406–412, 1995.

18. Coves, A., B. Gimeno, A. A. San Blas, A. Vidal, V. E. Boria, and M. V. Andres, "Three-dimensional scattering of dielectric gratings under plane-wave excitation," *IEEE Antennas Wireless Propag. Lett.*, Vol. 2, 215–218, 2003.

19. Brundrett, D. L., E. N. Glysis, and T. K. Gaylord, "Homogeneous layer models for high-spatial-frequency dielectric surface-relief gratings: Conical diffraction and antireflection designs," *Appl. Opt.*, Vol. 33, 2695–2706, 1994.

20. Moharam, M. G., E. B. Grann, D. A. Pommet, and T. K. Gaylord, "Formulation for stable and efficient implementation of the rigorous coupled-wave analysis of binary gratings," *J. Opt. Soc. Am. A*, Vol. 12, 1068–1076, 1995.

21. Moharam, M. G., D. A. Pommet, E. B. Grann, and T. K. Gaylord, "Stable implementation of the rigorous coupled-wave analysis for surface-relief gratings: Enhanced transmittance matrix approach," *J. Opt. Soc. Am. A*, Vol. 12, 1077–1086, 1995.

22. Gimeno, B., J. L. Cruz, E. A. Navarro, and V. Such, "A polarizer rotator system for three-dimensional oblique incidence," *IEEE Trans. Antennas Propag.*, Vol. 42, 912–919, 1994.

23. Silvestre, E., M. V. Andres, and P. Andres, "Biorthonormal-basis method for the vector description of optical-fiber modes," *J. Lightwave Technol.*, Vol. 16, 923–928, 1998.

24. Ferrando, A., E. Silvestre, J. J. Miret, P. Andres, and M. V. Andres, "Full-vector analysis of a realistic photonic crystal fiber," *Opt. Lett.*, Vol. 24, 276–278, 1999.

25. Coves, A., B. Gimeno, J. Gil, M. V. Andres, A. A. San Blas, and

V. E. Boria, "Full-wave analysis of dielectric frequency-selective surfaces using a vectorial modal method," *IEEE Trans. Antennas Propag.*, Vol. 52, 2091–2099, 2004.

26. Harrington, R. F., *Field Computation by Moment Methods*, IEEE Press, USA, 1993.

27. Coves, A., B. Gimeno, D. Camilleri, M. V. Andres, A. A. San Blas, and V. E. Boria, "Scattering by dielectric frequency-selective surfaces using a vectorial modal method," *Proceedings of IEEE AP-S Int. Symp. and URSI National Radio Sci. Meeting*, 580–583, San Antonio, TX, USA, 2002.

28. Collin, R. E., *Field Theory of Guided Waves*, 2nd Edition, IEEE Press, New York, 1991.

29. Chu, T. S. and T. Itoh, "Generalized scattering matrix method for analysis of cascaded and offset microstrip step discontinuities," *IEEE Trans. Microwave Theory Tech.*, Vol. 34, 280–284, 1986.

30. Wang, S. S. and R. Magnusson, "Theory and applications of guided-mode resonance filters," *Appl. Opt.*, Vol. 32, 2606–2613, 1990.

31. Ding, Y. and R. Magnusson, "Use of nondegenerate resonant leaky modes to fashion diverse optical spectra," *Opt. Express*, Vol. 12, 1885–1891, 2004.

32. Ding, Y. and R. Magnusson, "Resonant leaky-mode spectral-band engineering and device applications," *Opt. Express*, Vol. 12, 5661–5674, 2004.

33. Shokooh-Saremi, M. and R. Magnusson, "Wideband leaky-mode resonance reflectors: Influence of grating profile and sublayers," *Opt. Express*, Vol. 16, 18249–18263, 2008.

34. Snyder, A. W. and J. D. Love, *Optical Waveguide Theory*, Chapman and Hall, London, 1983.